Rapid generation of regionally specified CNS neurons by sequential patterning and conversion of human induced pluripotent stem cells

Chen, Muwan; Maimaitili, Muyesier; Habekost, Mette; Gill, Katherine P; Mermet-Joret, Noëmie; Nabavi, Sadegh; Febbraro, Fabia; Denham, Mark

Published in:
Stem Cell Research

DOI (link to publication from Publisher):
10.1016/j.scr.2020.101945

Publication date:
2020

Document Version
Publisher's PDF, also known as Version of record

Stem Cell Research 48 (2020) 101945

Contents lists available at ScienceDirect

Stem Cell Research

journal homepage: www.elsevier.com/locate/scr

Rapid generation of regionally specified CNS neurons by sequential patterning and conversion of human induced pluripotent stem cells

Muwan Chen[a,b], Muyesier Maimaitili[a,b], Mette Habekost[a,b], Katherine P. Gill[a,b], Noëmie Mermet-Joret[a,c], Sadegh Nabavi[a,c], Fabia Febbraro[a,d], Mark Denham[a,b,*]

[a] Danish Research Institute of Translational Neuroscience (DANDRITE), Nordic EMBL Partnership for Molecular Medicine, Aarhus University, Denmark
[b] Department of Biomedicine, Aarhus University, Denmark
[c] Department of Molecular Biology and Genetics, Aarhus University, Denmark
[d] Department of Health Science and Technology, Aalborg University, Denmark

ARTICLE INFO

Keywords:
Induced pluripotent stem cells
Direct conversion
Patterning
Cortical neurons
V2a interneuron

ABSTRACT

The differentiation of patient-specific induced pluripotent stem cells (iPSCs) into specific neuronal subtypes has been exploited as an approach for modeling a variety of neurological disorders. However, achieving a highly pure population of neurons is challenging when using directed differentiation methods, especially for neuronal subtypes generated by complex and protracted protocols. In this study, we efficiently produced highly pure populations of regionally specified CNS neurons by using a modified NGN2-Puromycin direct conversion protocol. The protocol is amenable across a range of iPSC lines, with more than 95% of cells at day 21 positive for the neuronal marker MAP2. We found that conversion from pluripotent stem cells resulted in neurons from the central and peripheral nervous system; however, by incorporating a short CNS patterning step, we eliminated these peripheral neurons. Furthermore, we used the patterning step to control the rostral-caudal identity. This approach of sequential patterning and conversion produced pure populations of forebrain neurons, when patterned with SMAD inhibitors. Additionally, when SMAD inhibitors and WNT agonists were applied, the approach produced anterior hindbrain excitatory neurons and resulted in a neuronal population containing VSX2/SHOX2 V2a interneurons. Overall, this sequential patterning and conversion protocol can be used for the production of a variety of CNS excitatory neurons from patient-derived iPSCs, and is a highly versatile system for investigating early disease events for a range of neurological disorders including Alzheimer's disease, motor neurons disease and spinal cord injury.

1. Introduction

Since the derivation of induced pluripotent stem cells (iPSCs), patient-specific iPSCs have been produced from a broad range of patients with sporadic or familial forms of neurological diseases. When combined with gene editing techniques to correct or introduce mutations, the diseased and isogenic iPSCs can be used together to investigating disease mechanisms *in vitro*. A constant focus in the field has, therefore, been towards the development of differentiation protocols that can more closely recapitulate sequential *in vivo* patterning events and direct cell fate towards specific brain regions, in order to generate appropriate neuronal subtypes for modeling a neurological disease (Arenas et al., 2015; Davis-Dusenbery et al., 2014). One of the current challenges in the field is that directed differentiation protocols take several weeks or even months to produce high percentages of post-mitotic neurons, the cells become more asynchronous as the protocol becomes more protracted, and cultures come to contain varying amounts of progenitor cells at differing maturity. These restraints hamper the use of high-throughput analyses or sequencing methods. Several approaches have been adopted to remove progenitors or accelerate their differentiation to a mature neuronal state. However, accelerated differentiation using various combinations of inhibitors has only been successful at producing a limited range of neuronal subtypes of either forebrain or sensory neurons, depending on the inhibitors used (Chambers et al., 2012; Qi et al., 2017; Telezhkin et al., 2016).

An alternative to directed differentiation is direct reprogramming, which can be performed from fibroblasts or other somatic cells and is capable of directly generating post-mitotic neurons (Ambasudhan et al., 2011; Chanda et al., 2014; Vierbuchen et al., 2010). Applying this method to pluripotent stem cells overcomes limitations in the

* Corresponding author at: Department of Biomedicine, Aarhus University, Høegh-Guldbergs Gade 10, Building 1116, Aarhus 8000 C, Denmark.
E-mail address: mden@dandrite.au.dk (M. Denham).

https://doi.org/10.1016/j.scr.2020.101945
Received 11 December 2019; Received in revised form 27 July 2020; Accepted 30 July 2020
Available online 03 August 2020

availability of precious patient cells and, when combined with a resistance gene to select for transgene expression, the method can result in a highly pure population of excitatory neurons (Chanda et al., 2014; Pang et al., 2011; Thoma et al., 2012; Zhang et al., 2013). Conversion to alternate neuronal lineages can also be achieved by supplementing the neuronal conversion genes with lineage-specific transcription factors. However, the inclusion of multiple conversion factors to generate alternate neuronal subtypes introduces additional inefficiencies and requires an understanding of which transcription factor determinants are specifically required for each lineage (Blanchard et al., 2014; Pfisterer et al., 2011; Son et al., 2011; Theka et al., 2013). Having the ability to directly convert cells to a broader range of neurons without the need to identify a specific transcription factor determinate would considerably increase the applicability of direct conversion as a method to generate neurons for disease modeling.

In this study, we sought to develop a platform for converting iPSCs into region-specific neurons. By combining the early patterning events of a differentiation protocol with a direct conversion approach, we produced highly pure, regionally specified induced neurons (iNs). To achieve this, we began by optimising an NGN2-Puromycin direct conversion protocol to produce pure populations of excitatory neurons. We demonstrated that optimisation of the antibiotic selection period and concentration enables highly pure neuronal cells to be obtained, and the addition of mitotic inhibitors can be avoided, resulting in a protocol that is amenable across a broad range of iPSC lines. Interestingly, the NGN2-conversion from the pluripotent state yielded a mixed neuronal culture containing a significant number of peripheral neurons. To overcome this and have the ability to control the differentiation towards specific central nervous system (CNS) fates, we incorporated a short differentiation-patterning step that successfully prevented the generation of peripheral neurons. By using factors known to alter the rostral-caudal identity, we successfully specified the neurons to specific brain regions and produce pure populations of either forebrain or anterior hindbrain excitatory neurons. Thus, this approach can produce regionally specified post-mitotic CNS excitatory neurons from patient-derived iPSCs, which stands as a highly relevant system for investigating a range of neurological disorders.

2. Materials and methods

2.1. Human pluripotent stem cell culture

The following iPSCs lines were used in this study: CCD-001-C3 (DANi-001C), GBA-002-C3 (DANi-002C), GBA-003-C8 (DANi-003H), PRKN-004-C1 (DANi-004A), LRRK2-GBA-005-C1 (DANi-005A), GBA-006-C6 (DANi-006F), PINK1-007-C1 (DANi-007A), SNCA-008-C6 (DANi-008F), SNCA-009-C3 (DANi-009C), GBA-010-C1 (DANi-010A), LRRK2-011-C1 (DANi011-A) (Chen et al., 2020a, 2020b). Additionally, human embryonic stem cells (hESCs) H9 (WA-09, WiCell) were included. Pluripotent stem cells were cultured on irradiated human foreskin fibroblasts (HFF; ATCC CRL-2097) in KSR media consisting of DMEM/nutrient mixture F-12, supplemented with β-mercaptoethanol 0.1 mM, non-essential amino acids (NEAA) 1%, glutamine 2 mM, penicillin 25 U/ml, streptomycin 25 U/ml and knockout serum replacement 20% (all from Life Technologies), supplemented with FGF2 (15 ng/ml; Peprotech) and Activin A (15 ng/ml; R&D systems). Colonies were mechanically dissected every 7 days and transferred to freshly prepared HFF. Media was changed every second day. Prior to differentiation, PSCs were expanded feeder-free in TESR-E8 media on Vitronectin XF™ (STEMCELL Technologies). All cells were cultured at 37 °C and 5% CO_2.

2.2. Lentiviral production

Lentiviruses were produced in HEK293T/17 (ATCC; CRL-11268) cells by co-transfection with three plasmids: a packaging plasmid (psPAX2), envelope plasmid (pMD2.G) and a vector plasmid (FUW-M2rtTA or pTet-O-Ngn2-puro or pTet-O-NGN2-puro-GFP) all acquired from Addgene (12260, 12259, 20342, 52047, 79823, respectively). 15 μg of packaging plasmid, 5 μg of envelope plasmid, 20 μg of vector plasmid were transfected per 55 cm^2 culture dish using Lipofectamine 3000 (Life Technologies). Viral supernatant was harvested with DMEM medium supplemented with 5% KSR, 1% glutamax, 1% penicillin/streptomycin, 0.5% HEPES (all from Life Technologies) over two days. On the second day, viral supernatant was centrifuged for 10 min at 500g and filtered through a 0.45 μm filter and pelleted by ultracentrifugation (91,000 g for 90 min at 4 °C) through a sucrose cushion (20% sterile sucrose in TNE buffer containing 50 mM Tris-HCl (pH 7.4), 100 mM NaCl, 0.5 mM ethylenediaminetetraacetic acid (EDTA)). Then, the viral pellets were resuspended in ice-cold Neurobasal medium (Life Technologies), aliquoted and frozen on dry-ice, stored at −80 °C for future use.

2.3. Direct conversion of human ESCs and iPSCs into induced neurons (iNs)

Human ESCs or iPSCs were expanded on a Vitronectin-coated (STEMCELL Technologies) 35 mm diameter Petri dish (Thermo scientific) in TeSR™-E8™ basal medium (STEMCELL Technologies). When the cells reached 70–80% confluence, they were dissociated with Gentle Cell Dissociation Reagent (STEMCELL Technologies), and Y-27632 (10 μM, Tocris Bioscience) was added to the medium for 12 h post-dissociation. The protocol of direct conversion of human ESCs and iPSCs into induced neurons (iNs) is shown in Fig. 1A. Two days before neural conversion (day −2), 250,000 cells of H9 or iPSCs were plated on a Vitronetin-coated 35 mm diameter Petri dish in TeSR-E8 basal medium with 10 μM of Y-27632. On day −1, cells were transduced with lentivirus FUW-M2rtTA and either Tet-O-Ngn2-puro or Tet-O-Ngn2-puro-GFP with a total MOI of 50. On day 0, the culture medium was replaced with N2B27 media containing 1:1 of Neurobasal medium (NBM) and DMEM/F-12 supplemented with N2 supplement 1%, B27 Supplement Minus Vitamin A 1%, insulin/transferrin/selenium-A (ITS-A) 1%, glucose 0.3%, glutamax supplement 1%, penicillin/streptomycin 0.5% (all from Life Technologies) and doxycycline (1 μg/mL; Sigma-Aldrich) to induce TetO gene expression. On day 2, puromycin (3 μg/mL; Gibco) selection began. On day 5, surviving neural progenitors were dissociated with StemPro Accutase Cell Dissociation Reagent (Life technologies) with DNase (0.1 mg/ml, Sigma-Aldrich) and replated on poly-L-ornithine (0.1 mg/mL), laminin (10 μg/mL) and fibronectin (10 μg/mL) (all from Sigma-Aldrich) triple-coated plastic wells or glass coverslips at a density of 120,000 cells/cm^2 in Neurobasal medium supplemented with B27 2%, penicillin/streptomycin 0.5%, ascorbic acid (200 μM; Sigma-Aldrich), DAPT (2.5 μM; Tocris), doxycycline (1 μg/mL), and puromycin (3 μg/mL). On day 7, puromycin was removed from the culture media. Media was changed every 2 days and samples were collected on day 14 or day 21.

2.4. Differentiation prior to direct conversion

hESCs and two iPSCs (GBA-002-C3 and GBA-006-C6) were used for patterning experiments. For forebrain patterning, cells were cultured in N2B27 media and supplemented with SB431542 (SB; 10 μM, Tocris Bioscience) and LDN193189 (LDN; 100 nM, Stemgent) for 6 days before direct conversion, referred to as SB-LDN-NGN2. For hindbrain patterning, N2B27 media was supplemented with 10 μM SB and CHIR99021 (CHIR; 3 μM, Stemgent) for 4 days before direct conversion, referred to as SB-CHIR-NGN2. Samples were collected on day 21 for immunostaining.

2.5. Immunolabeling

Cell culture dishes or coverslips were blocked for 1 h at room temperature in blocking solution consisted of 5% donkey serum in PBT

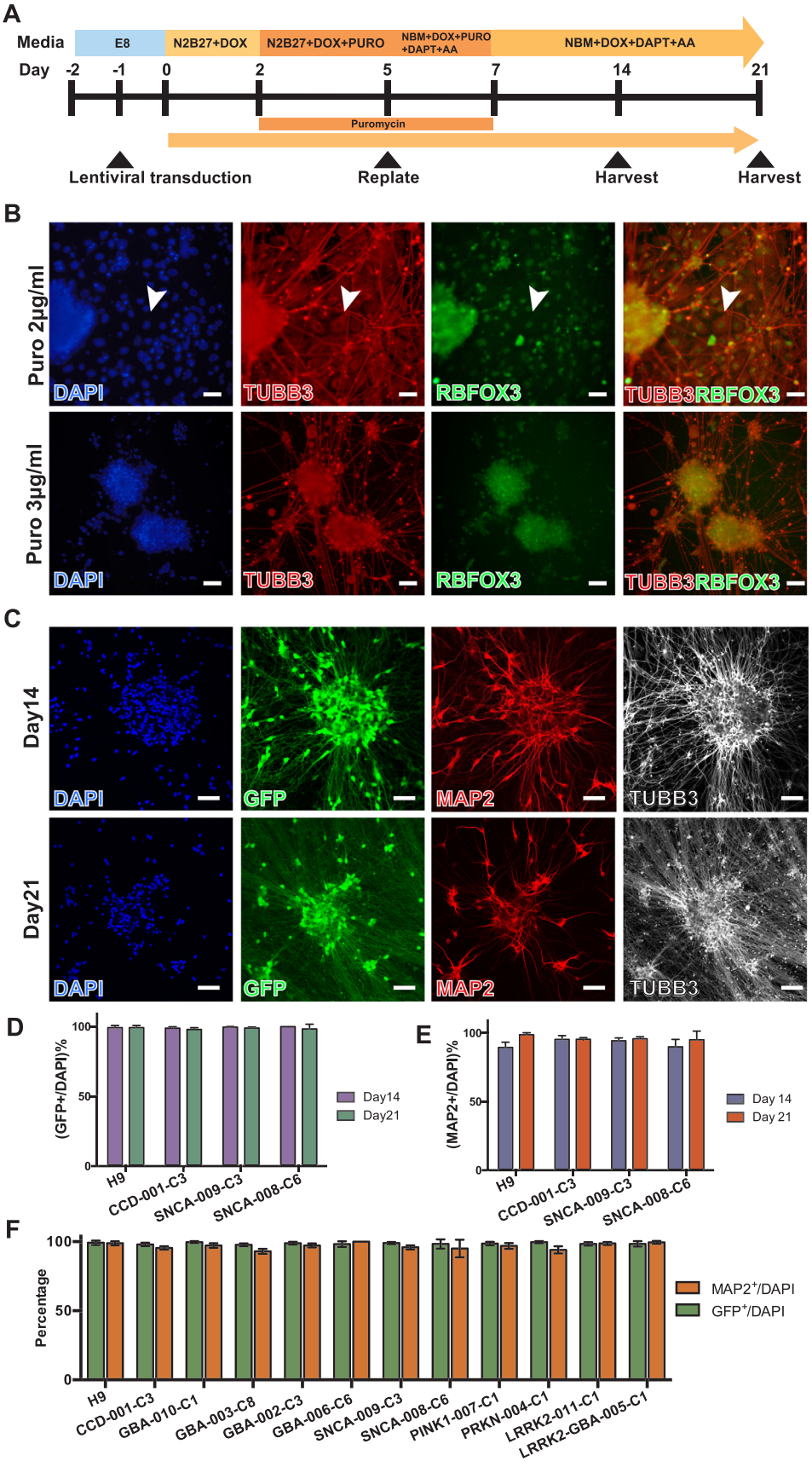

Fig. 1. Generation of induced neurons (iNs) by direct conversion of human induced pluripotent stem cells. (A) Schematic diagram of the induced neuron protocol. DOX: doxycycline, PURO: puromycin, AA: ascorbic acid. (B) Immnuostaining of iNs on day 14 with different concentrations of puromycin. Blue: DAPI, Green: RBFOX3, Red: TUBB3. Arrowheads point to RBFOX3 positive non-neuronal cells. Bar = 50 μm. (C) Representative images of iNs with over-expression of NGN2-EGFP and immunostaining of neuronal markers MAP2 and TUBB3. Bar = 50 μm. (D) The transduction efficiency of the protocol (4 different cell lines) on day 14 and day 21. (E) The maturation rate of iNs (4 different cell lines) on day 14 and day 21 by calculating the MAP2-postive cells, compared to DAPI staining. (F) The transduction and maturation efficiency of iNs for the hESC line and all of the hiPSC lines (12 different cell lines) on day 21. Data are showed as the mean ± S.D (n = 4).

(PBS with 0.25% triton-X) solution. The following primary antibodies were used: mouse anti-TUBB3 (Millipore, MAB1637: 1:1000), rabbit anti-TUBB3 (Biolegend, 802001, 1:1000), mouse anti-NeuN (RBFOX3; Millipore, MAB377, 1:500), chicken anti-MAP2 (Abcam, ab92434, 1:2500), guinea pig anti-synaptophysin 1 (Synaptic Systems, 101004, 1:1000), mouse anti -PSD95 (Abcam, ab2723, 1:500), rabbit anti-vGLUT2 (SLC17A6; Synaptic Systems, 1:500), mouse anti-peripherin (PRPH, Millipore, MAB1527, 1:500), rabbit anti-TBR1 (Abcam, ab31940, 1:200), mouse anti-NEUROG3 (DSHB, F25A1B3, 1:4), sheep anti-CHX10 (VSX2, Abcam, AB16141, 1:200), mouse anti-SHOX2 (Abcam, ab55740, 1:500). Antibodies were diluted in blocking solution incubated on sections and cultures overnight at 4 °C. Following three 10-minute washes in PBT, the corresponding secondary antibodies were applied for 1 h at room temperature. For mouse anti-PSD95 antibody, second antibody was applied with biotin anti-mouse (Jackson ImmunoResearch, 715-065-150, 1:200), followed by Alexa Fluor 488 Streptavidin (Jackson ImmunoResearch, 016-540-084, 1:1000). Nuclei were counterstained with 4́, 6-diamidino-2-phenylindole (DAPI; 1 μg/ml, Sigma). Slides were mounted in PVA-DABCO for viewing under a fluorescent microscope (ZEISS ApoTome), and images captured using the ZEN software. Confocal microscopy was performed using a ZEISS LSM 780 Confocal Microscope.

2.6. Electrophysiology

For the electrophysiological recordings, iNs were replated on individual 13 mm coverslips (VWR, Ø 13 mm) on day 5 following an additional 8 weeks of maturation time. The iNs on the coverslips were transferred into a recording chamber and continuously perfused with Artificial Cerebrospinal Fluid containing (in mM): NaCL 119, KCl 2.5, NaHCO3 26, 1 NaH2PO4, D-glucose 11, CaCl2 2, MgCl2 2, adjusted to pH 7.4 and bubbled with a mixture of CO2 (5%) and O2 (95%), at room temperature. The chamber was mounted on an upright microscope (Scientifica) linked to a digital camera (QImaging Exi Aqua) and the cells were visualized using 63X water-immersion objective (Olympus). Acquisitions were performed in a whole-cell configuration using Clampex 10.6 software connected to a Multiclamp 700B amplifier via a Digidata 1550A digitizer (all from Molecular Devices). Voltage-clamp data were low-pass filtered at 200 Hz and digitized at 10 kHz and the whole-cell capacitance was compensated. Patch pipettes (3–7 MΩ of resistance) were filled with internal solution containing (in mM): K-gluconate 170, Hepes 10, NaCl 5, KCl 10, EGTA 0.6, Na2GTP 2, and NaGTP 0.3. The pH and osmolarity of the internal solution were close to physiological conditions (pH 7.25, osmolarity 285 mOsm). The access resistance of the cells in our sample was ~ 19 MOhm. Spontaneous excitatory postsynaptic currents (sEPSC) were recorded in voltage-clamp gap-free mode (clamped at −65 mV). Current-clamp mode was used to analyse the intrinsic firing properties of the cell. Briefly, repetitive depolarizing current pulses (800 ms) of incremental amplitude (10 pA) were used to determine the rheobase corresponding to the minimum depolarizing current intensity needed to generate an action potential (AP). Amplitude and spike-width of APs were measured on the first AP at the rheobase level. Repetitively firing neurons were defined as those capable of firing ≥ 3 APs in response to a depolarizing current step. The amplitude of APs was measured from the point preceding the fast rising phase of the spike to the peak of the spike, whereas APs duration was defined as the width at half-maximal spike amplitude. Data analysis was performed by Clampfit 10.6 (Molecular device). Data are shown as the mean ± S.E.M.

2.7. RNA sequencing and analysis

For RNA sequencing, we used the hESC line and differentiated them into the three iN groups NGN2, SB-CHIR-NGN2 and SB-LDN-NGN2 and extracted RNA at day 21. RNA from undifferentiated hESCs were collected and used as a control. Three biological replicates from each group were collected, resulting in a total of 12 samples sequenced. Specifically, RNA was extracted using RNeasy Mini Kit (Qiagen) following the manufacture's instruction, and sent to BGI-China for mRNA library construction, which consisted of mRNA enrichment by oligo dT selection using magnetic beads. RNA was fragmented and reverse transcribed to cDNA by N6 random primers. cDNA was amplified by PCR and single-end sequencing performed with a minimum of 20 M clean reads acquired per sample on a BGISEQ500 platform. Bioinformatic analysis followed standard procedures of removing adaptors, mapping to the reference human genome (hg19) using HISAT and Bowtie2 tools, and differential gene expression detected using DEseq2. For principal component analysis, the full transcriptomic profile (21,774 genes) was included for analysis. Principal components were calculated by singular value decomposition of the centred and scaled data matrix using the prcomp function in R stats package. Heatmaps were generated by log2 transforming and mean scaling FPKM values of selected genes using heatmap.2 function in R stats package. A Venn diagram was constructed using differentially expressed genes (adjusted p-value lower than 0.05) identified by comparison of NGN2, SB-LDN-NGN2 or SB-CHIR-NGN2 group to hESCs. Bar graphs of the top 10 significantly up/down-regulated genes present Log2 (Fold Change) values of differentially expressed genes, identified by comparison of SB-LDN-NGN2 or SB-CHIR-NGN2 group to NGN2. Threshold bar (white line) indicates a fold change of ± 2. RNAseq data reported in this paper is deposited in the Gene Expression Omnibus (GEO) with accession number GSE149864.

2.8. Multi-electrode array (MEA) recording and analysis

Three groups of iNs were plated on day 5 with a density of 100,000 cells/well on poly-L-ornithine (0.1 mg/mL), laminin (10 μg/mL) and fibronectin (10 μg/mL) (all from Sigma-Aldrich) triple-coated 24-well MEA plate (Multi Channel Systems MCS GmbH) in Neurobasal medium supplemented with B27 2%, penicillin/streptomycin 0.5%, ascorbic acid (200 μM; Sigma-Aldrich), DAPT (2.5 μM; Tocris), doxycycline (1 μg/mL), and BDNF (20 ng/ml; R&D systems). Since there was no obvious spontaneous activities detection on the day 21 culture for the NGN2 group, human astrocytes (Sciencell) were added with a density of 25,000 cells/well to support the culture system for electrophysiological recordings for the all the three groups. Spontaneous firing was recorded for two minutes each time, twice a week for up to 10 weeks with Multiwell-Screen software (Multi Channels Systems MCS GmbH). Signals were sampled at 20 kHz and low-pass Butterworth filterer cutoff was 3500 Hz and high-pass Butterworth filter cutoff was 100 Hz. Data analysis were performed with Multiwell-Analyzer software (Multi Channels Systems MCS GmbH). A spike detection was recorded when signal exceeded a threshold of ± 5% of standard deviation of the baseline noise during quiescent periods. A burst detection was recorded following these settings: maximum interval to start and end burst was 50 ms; the minimum interval between bursts was 100 ms; the minimum duration of burst was 50 ms, and there were more than 4 spikes counts in a burst. A network burst detection was recorded when minimum 6 channels participating and minimum simultaneous channels are 3.

To investigate pharmacological effects, synaptic antagonists were added to the neuronal culture media. The AMPA/kainite receptor antagonist 2,3-Dioxo-6-nitro-1,2,3,4-tetrahydrobenzo(f)quinoxaline-7-sulfonamide (NBQX, 10 μM, Tocris) and sodium ion/channel antagonist tetrodotoxin (TTX, 1 μM, Tocris) were added into separated MEA wells. Spontaneous firing was recorded before and 30 mins after NBQX treatment and 5 mins after TTX treatment.

3. Results

3.1. Direct conversion to iNs from human ESCs or iPSCs

Previous studies have demonstrated that direct conversion of hESCs

or iPSCs into neurons can be achieved via a single proneural transcription factor (Chanda et al., 2014; Goparaju et al., 2017). NeuroD1 or NGN2, are among the most potent; ASCL1, whilst also effective, has been reported to have a slower conversion rate (Goparaju et al., 2017; Zhang et al., 2013). We, therefore, selected NGN2 as the conversion factor in our study and first sought to determine its robustness at converting human iPSCs into neurons. By lentiviral delivery, we overexpressed either NGN2 and Puromycin N-acetyl transferase or NGN2, EGFP and Puromycin N-acetyl transferase; both constructs contain a doxycycline inducible tetO promoter (Zhang et al., 2013). Two days after lentiviral transduction, a high percentage of cells were EGFP positive, with only a few non-transduced EGFP negative cells present (Supplementary Fig. 1A). Despite the high transduction rate, cells without puromycin selection showed a vast difference in cellular morphology by day 7 and only a few cells presented with a neuronal morphology (Supplementary Fig. 1B). Conversely, after five days of puromycin selection at 2 μg/ml, we observed an abundance of neurons; intriguingly, however, RBFOX3 positive cells with a non-neuronal morphology were present within these cultures (Fig. 1B). To prevent the appearance of these non-neuronal cells, we first tested a range of puromycin concentrations, up to 10 μg/ml. We determined that after five days of puromycin selection, a concentration of 3 μg/ml was sufficient to dramatically reduce the presence of non-transduced cells (EGFP negative) and non-neuronal RBFOX3 positive cells in the culture by day 7.

Secondly, we included a replating step to further enhance the purity of converted cells (Supplementary Fig. 1C-D). The percentage of EGFP positive cells at a replating density of 250,000 cells/cm^2 on day 7 was 89.84% ± 4.13 S.D. Decreasing the plating density to 120,000 cells/cm^2 resulted in no detectable EGFP negative cells. By combining the optimised puromycin concentration and replating density, we efficiently and reproducibly converted all iPSC lines to neurons (Fig. 1C-F). Across all the different lines, the percentage of transduced cells on day 14 and day 21 was above 97.93% ± 1.31 S.D (Fig. 1D). The neuronal marker MAP2 increased slightly from day 14 to day 21, all lines were above 89.51% ± 3.84 S.D at day 14, and above 95.06% ± 6.38 S.D at day 21 (Fig. 1E).

3.2. Electrical activity of the converted neurons

Whole-cell electrophysiological recordings confirmed that the neurons exhibited neuronal activity, indicative of mature, functional neurons. At days 84–86, the recorded neurons showed sEPSC, with an average amplitude of 46,0 ± 11,4 pA and a frequency of 20,4 ± 4,9 events per minute, confirming the formation of excitatory synapses (Fig. 2A). The cells' intrinsic membrane properties were also measured as an indication of a functional maturation: the membrane resistance was 500,8 ± 138,2 MOhm, and mean capacitance was 39.90 ± 5.28 pF (Fig. 2B). We then asked if the cells were able to fire action potentials (APs) in response to the injection of current, and observed that repetitive firing can be induced in sufficiently depolarized cells. In our experiment, the injected current necessary to induce a first AP (i.e, rheobase, red trace) was 27.5 ± 6.3 pA (Fig. 2C). The rheobase was directly linked to the resting membrane potential of the cell (Vm). At days 84–86, the Vm of our recorded cells was −50,5 ± 4,1 mV (Fig. 2D). Detailed analysis of AP properties revealed a mature shape of the APs, with a discharge threshold (APthresh) of −31.6 ± 1.9 mV, AP amplitude averaged 38.5 ± 8.0 mV, and a half-width of 6.5 ± 1.7 ms (Fig. 2D). Finally, we saw that the cells responded by an increase in the number of APs to an increment of the amplitude of the current injected (Fig. 2D).

3.3. Combining differentiation and direct conversion to generate pure CNS neurons

Having optimised an efficient neuronal conversion method, we then further characterised the types of neurons generated from the Ngn2-conversion protocol. In agreement with our electrophysiological recordings, the iNs displayed punctate staining for both synaptophysin (SYP) and postsynaptic protein PSD-95, which indicates synaptic maturity (Fig. 3A). Furthermore, we observed the expression of neuronal marker RBFOX3 (Fig. 3B) and glutamate transporter SLC17A6 (VGLUT2) in the neurons (Fig. 3C). We could not detect GABA or TH-positive neurons, or astrocytes (GFAP-positive; data not shown), although interestingly, a population of peripheral neurons was observed in the cultures (Fig. 3D). The percentage of PRPH$^+$/DAPI neurons was 9.40% (± 3.29 S.D), 10.24% (± 3.05 S.D), and 9.20% (± 3.55 S.D) across three different cell lines.

To prevent the presence of peripheral neurons, we incorporated a short differentiation step before the direct conversion protocol (Fig. 4A). Two differentiation methods were developed that patterned the hESCs/iPSCs into neural progenitors of either the forebrain or hindbrain. For forebrain specification we patterned the cells with SB431542 and LDN193189 referred to as SB-LDN-NGN2 and for hindbrain patterning we used SB431542 and CHIR99021, referred to as SB-CHIR-NGN2. Previously, we reported both of these patterning methods to successfully differentiate iPSCs to NSCs of these regions (Chen et al., 2018; Denham et al., 2015, 2012). Regardless of the patterning, upon neuronal conversion and selection, the two new protocols produced neurons with high efficiency similar to the NGN2 group. We next used RNAseq to determine how the patterning had altered their neuronal identity. Firstly, gene expression from all the samples was normalized and compared using principal component analysis (Fig. 4B). We observed that PC1 had the highest variance (50.7%) and revealed a clear separation between the undifferentiated stem cell state and the neuronal groups, whereas PC2 could separate the neuronal groups based on anterior-posterior identity: the SB-CHIR-NGN2 group separated from the NGN2 and SB-LDN-NGN2 groups with a variance of 18.1%. Within the four groups, we compared the expression of pluripotent genes (Fig. 4C). We observed that the pluripotent genes NANOG and POU5F1, as well as SOX2, were highly expressed in the hESCs group, but not in the three iN groups. Secondly, we examined the gene expression of neuronal lineage markers (Fig. 4D). As expected, all the three direct conversion groups, when compared to hESCs, expressed high levels of the mature neuronal markers SYP, DLG4, and MAP2, as well as higher levels of neuronal lineage markers (Fig. 4D). Uniquely to the NGN2 group, a high level of the peripheral neuronal marker PRPH was observed (Fig. 4D), which is in accordance with our immunostaining results (Fig. 3D). The inclusion of a patterning step, for both SB-LDN and SB-CHIR, significantly reduced the PRPH transcript levels (−4.14 log2 fold change of SB-LDN vs. NGN2 at a padj = 2.11×10^{-185} and −5.09 log2 fold change of SB-CHIR vs. NGN2 at a padj = 2.96×10^{-233}) and no PRPH positive cells could be identified by immunostaining in the SB-LDN or SB-CHIR groups (Supplementary Fig. 2). Compared to hESCs, all iN groups expressed significantly higher vesicular glutamate transporter SLC17A7 (SB-LDN padj = 3.50×10^{-38} and SB-CHIR padj = 1.77×10^{-39}) and SLC17A6 (SB-LDN padj = $1.02\text{x}10^{-282}$ and SB-CHIR padj = $4.12\text{x}10^{-143}$) levels, while very few transcripts were detected for GABA transporter SLC6A1 in SB-CHIR-NGN2 and SB-LDN-NGN2 groups, and no detectable transcripts were identified in any of the groups for GAD1 and GAD2 (< 1 FPKM).

We next examined the expression of anterior-posterior neuronal markers and forebrain markers. The SB-LDN-NGN2 group expressed the highest level of *SIX3* and *FOXG1* (Fig. 4C). The forebrain/midbrain marker *OTX2* was also higher in SB-LDN-NGN2 group, compared to NGN2 group and SB-CHIR-NGN2 group. At the midbrain level, the markers EN1 and PAX5 were not detected in any of the groups, and only very few transcripts for *PAX2* were detected in the NGN2 group (1.24 FPKM). At the hindbrain level, the SB-CHIR-NGN2 group expressed the highest level of *HOXA1* and *HOXA2* (Fig. 4C). For cervical, thoracic, lumbar and sacral markers; no transcripts were detected in the four groups. Gene expression comparisons showed that all three direct-

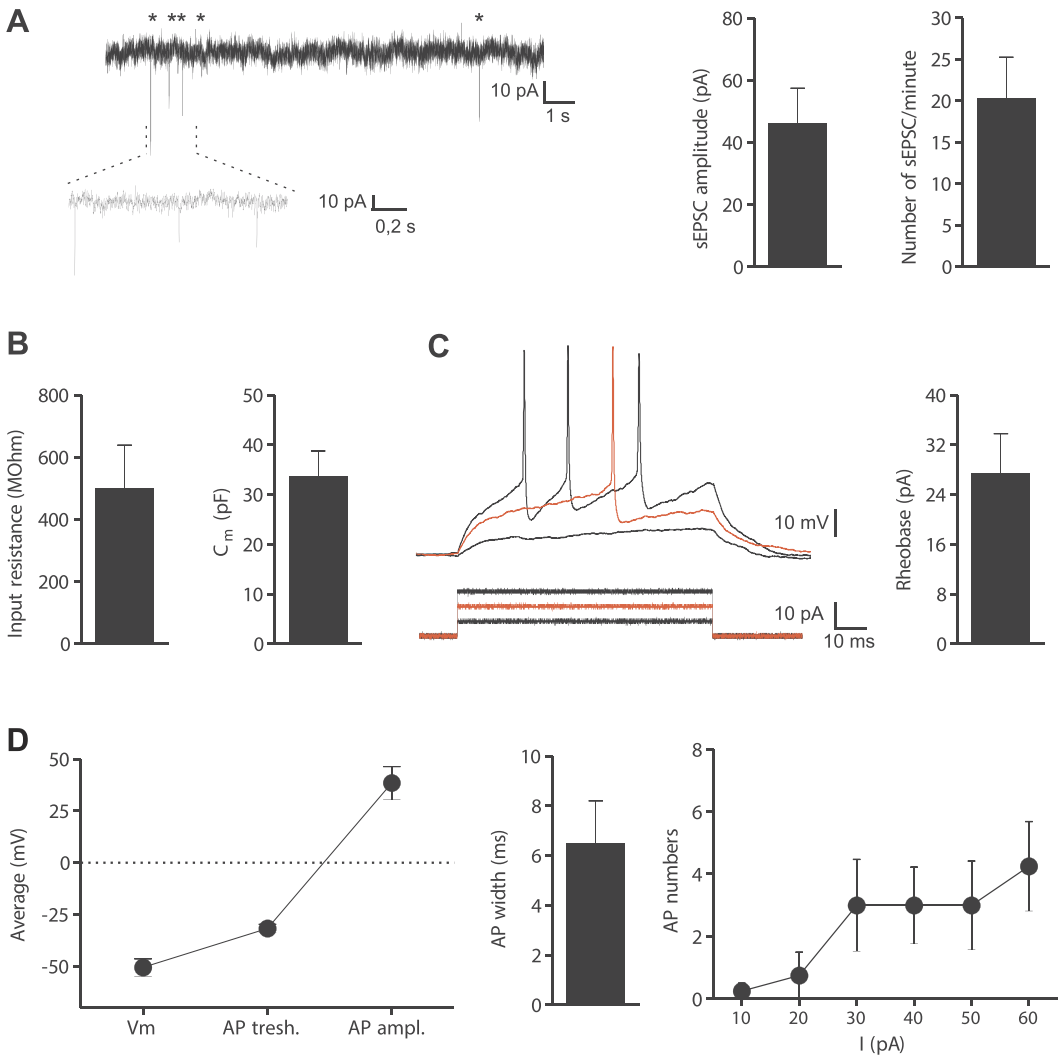

Fig. 2. Electrophysiological properties of iNs from iPSCs. (A) Representative trace of spontaneous excitatory postsynaptic currents (sEPSC, black stars) recorded at a holding potential of −65 mV in ACSF, with the amplitude and the frequency of the events. (B) Intrinsic membrane properties represented by the input resistance and the membrane capacitance (Cm). (C-D) Firing properties. (C) Representative traces of APs generated in response to a depolarizing current (lower trace). The rheobase (red trace) represent the injected-current necessary to induce the first APs. (D) The discharge threshold (APtresh.), the APs amplitude (APampl.), and the APs width were measured from the first evoked spike at the rheobase level. The number of APs was counted after each amplitude increment of step-current stimulation. Values are given as the mean ± S.E.M (n = 4).

converted groups shared 7650 genes (out of 12,264 genes) and, in accordance with PCA analysis, the SB-CHIR-NGN2 group contained the most unique genes (1793) from the other two neuronal populations, which accords with its more distinct hindbrain identity (Fig. 4E). The most differentially expressed genes were identified by direct comparison between the SB-CHIR-NGN2 group and the NGN2 group, as well as between the SB-LDN-NGN2 group and the NGN2 group (Fig. 4F). Of significance, in the SB-CHIR-NGN2 group, *VSX2* (previously known as CHX10), *NEUROG3*, *POU3F1*, and *SHOX2* were highly upregulated, while in the NGN2 group, *ISL1*, *NEUROG2* and *PRPH* were highly upregulated. In the SB-LDN-NGN2 group, *SIX3* and *FOXG1* were among the most differentially expressed genes (Fig. 4F). Overall, the results of the RNAseq analysis revealed that the SB-LDN-NGN2 group resulted in a forebrain cortical neuron identity, and that the SB-CHIR-NGN2 group resulted in a hindbrain identity.

VSX2 and *SHOX2* are both expressed in V2a interneurons, and both genes were highly expressed in the SB-CHIR-NGN2 group. V2b interneurons that express GATA3 are closely related to V2a interneurons, but *GATA3* was not detected in any of the groups. We were therefore interested in confirming the presence of V2a interneurons within the SB-CHIR-NGN2 group and, by immunostaining, we readily observed VSX2 and SHOX2 double-positive cells (Fig. 4G), with an efficiency of 43.17% ± 16.81 S.D, 45.83% ± 2.93 S.D, and 43.07% ± 8.97 S.D ($(VSX2^+SHOX2^+)$/DAPI)% for V2a interneurons converted from hESCs, GBA-006-C6, and GBA-002-C3 respectively. Immunostaining also confirmed that NEUROG3-positive cells featured prominently in SB-CHIR-NGN2, but not in NGN2 and SB-LDN-NGN2 (Fig. 4H). In the SB-LDN-NGN2 group, only a few SHOX2-positive neurons were observed and no VSX2-positive neurons were found. In the NGN2 group, neither VSX2 nor SHOX2 neurons were observed (Fig. 4G). Additionally, RNA *in situ* images (from the Allen Developing Mouse Brain Atlas in E11.5) of mouse embryos were used to confirm the spatial location of *Vsx2*, *Neurog3*, and *Shox2*, which identified these markers to be expressed in the ventral hindbrain and spinal cord, where V2a interneurons are located (Supplementary Fig. 3).

In the SB-LDN-NGN2 group, *TBR1* expression levels were significantly higher than in any of the other groups. To confirm its expression, we examined all neuronal conversion groups by immunostaining. We identified TBR1 in both the NGN2 and SB-LDN-NGN2 groups and not in the SB-CHIR-NGN2 group (Fig. 5). For the SB-LDN-NGN2 group, the efficiency of ($TBR1^+$/DAPI)% was 65.55% ± 4.16 S.D for hESCs and 62.84% ± 6.68 S.D for GBA-002-C3.

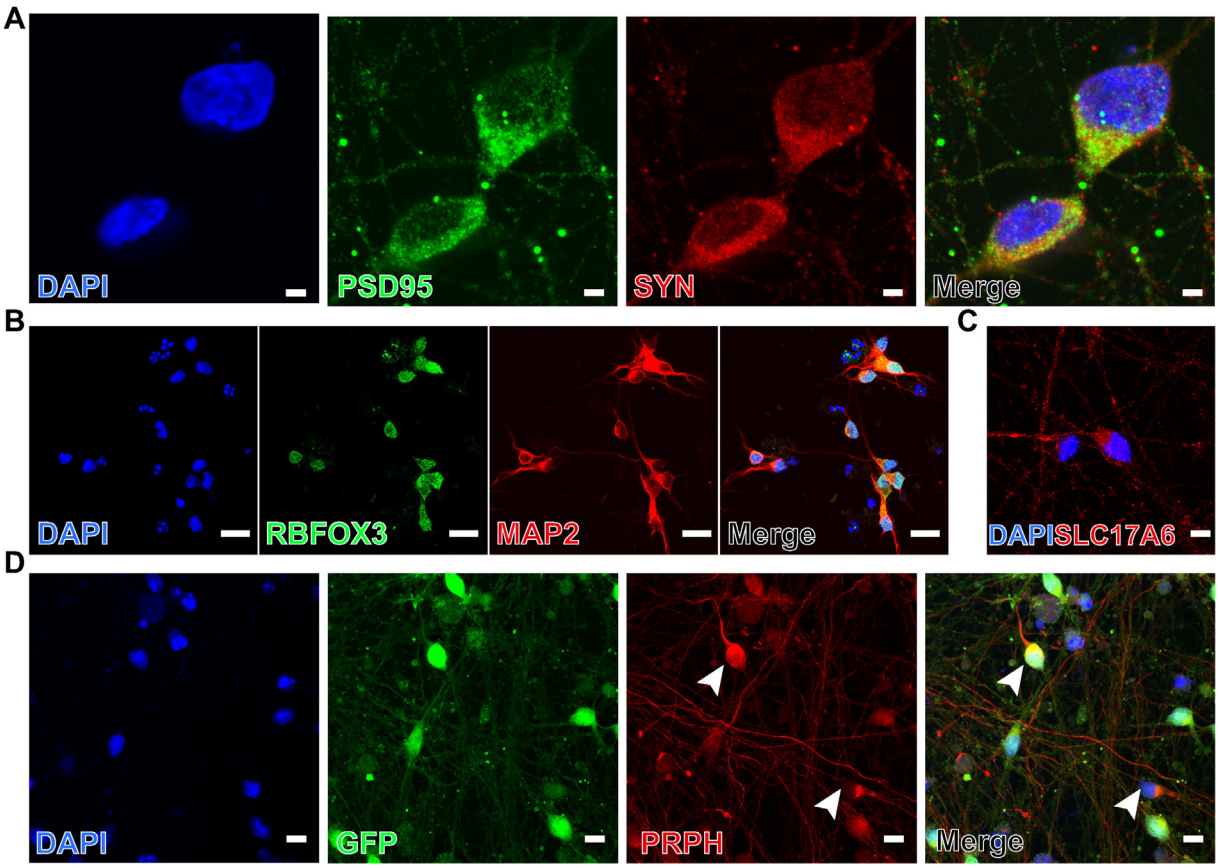

Fig. 3. Characterization of the iNs by immunostaining on day 21. (A) Representative images of DAPI, PSD95, and synaptophysin1 (SYN) staining. Bar = 2 μm. (B) Representative images of DAPI, RBFOX3 (NEUN), and MAP2 staining. Bar = 10 μm. (C) Representative images of DAPI and SLC17A6 (vGlut2) staining. Bar = 10 μm. (D) Representative images of DAPI, GFP, and PRPH staining. Arrowheads point to PRPH positive neurons. Bar = 10 μm.

3.4. Electrophysiological activity and functionality of the three iN groups by MEA

We used MEA to examine the electrophysiological activity of the neurons in all the three groups. We detected neural activity, recorded as spikes, first in the SB-CHIR-NGN2 group on day 16, and bursts and network bursts were seen on day 23. Following this, in the SB-LDN-NGN2 group, bursts were detected on day 30 and network bursts on day 54. The NGN2 group was the last group to show bursts (on day 33) with no network bust detection throughout the 65 days culture. On day 49, the SB-CHIR-NGN2 group showed a synchronized network burst with voltage around 400 μV. The SB-LDN-NGN2 group had network bursts with voltage around 50 μV. The NGN2 group had bursts but not network burst with the voltage around 30 μV (Fig. 6).

All the three iN groups responded to the treatment of AMPA/kainite glutamate receptor antagonist NBQX. The spontaneous firing decreased dramatically for both SB-CHIR-NGN2 and SB-LDN-NGN2 groups, while there were still some firing signals for the NGN2 group. With TTX treatment, the firing was eliminated from all the three groups (Supplementary Fig. 4).

4. Discussion

In this study, we established a robust and rapid protocol for generating regionally specified iNs from human iPSCs by combining a short patterning step with a direct conversion approach. We started out by examining the previously described NGN2-puromycin method, which has been shown capable of rapidly converting human iPSCs and hESCs into excitatory neurons with a cortical identity (Zhang et al., 2013). We determined that, in order to achieve a highly pure population of neurons, and to overcome variability in efficiencies between experiments and individual hiPSC lines, we needed to make several important modifications to the existing protocol.

We first optimised the concentration and duration of puromycin, as well as including a cell-replating step that further removed any remaining non-selected cells and dead cells and allowed for neurons to be replated at a consistent density, which was essential for the downstream transcriptomics and also provided a scalable and standard platform for converting numerous iPSCs lines in parallel.

After implementing these modifications, the percentage of transduced cells was above 97.93% (± 1.31) on day 14 and day 21, and the percentage of cells expressing the mature neuronal marker MAP2 was above 95.06% (± 6.38) (Fig. 1). Furthermore, we demonstrated that the neurons were synaptically mature: the 21-day culture contained SYP-positive synaptic punctate and PSD95 (Fig. 3A), and patch-clamp electrophysiology showed that neurons exhibited mature functional activity at 12 weeks of culture (Fig. 2). Overall, our replating step and puromycin optimisation successfully overcame the problem of cell line variability, ensured a consistent neuronal density at the end-point for all iPSC lines used, and resulted in functionally active neurons without the need to supplement the cultures with astrocytes, which thus ensured that the transcriptome analysis was purely from converted neurons.

Close examination of our NGN2 converted neurons revealed that peripheral neurons were present within the culture (Fig. 3D). To address this heterogeneity, we made a second modification to the protocol: we combined a differentiation/patterning step with the conversion to generate pure CNS neurons. Previous research has shown that hESCs can be patterned towards a forebrain identity with SMAD inhibition or towards a hindbrain fate by SMAD inhibition and activation

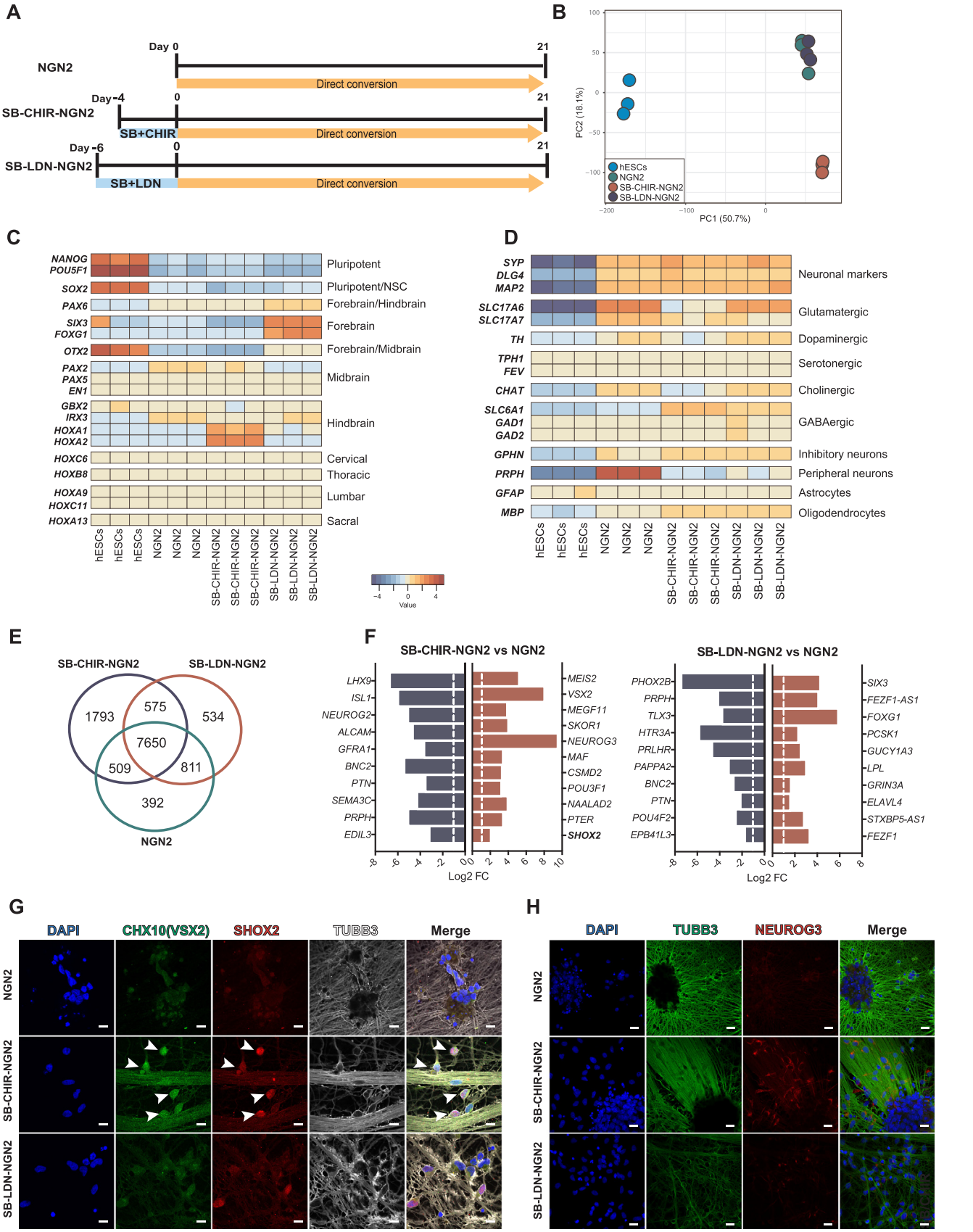

(caption on next page)

Fig. 4. Combining CNS patterning and direct conversion to generate pure CNS neurons. (A) Flow diagram of combining CNS patterning before the direct conversion protocol. (B) Principal component analysis shows a separation of the iNs groups from the undifferentiated stem cell state on PC1 and a separation of the iNs groups based on anterior-posterior identity on PC2. (C) Gene expression of known markers indicative of the pluripotent, anterior, and posterior patterning. (D) Gene expression of known markers indicative of neuronal lineages. (E) Schematic Venn diagram showing the overlap of genes within the three iNs groups. (F) The top 10 and selected additional (bold) downregulated (blue) and upregulated (red) genes in the CNS pre-patenting groups, versus the NGN2 group. Threshold bar (white line) indicates a fold change of ± 2. (G) Representative images of DAPI, VSX2, SHOX2 and TUBB3 staining. Arrowheads point to VSX2 and SHOX2 double positive cells. Bar = 10 μm. (H) Representative images of DAPI, TUBB3 and NEUROG3 staining. Bar = 20 μm. RNAseq data were from hESCs and hESC-derived iNs, immunostaining results were represented images from iNs converted from hESCs and two iPSCs lines.

of WNT signalling (Denham et al., 2015). We examined the effect of combining either of these two differentiation protocols with the NGN2-conversion approach. Our RNA sequencing analysis showed that both patterning steps, when followed by direct conversion, completely eliminated the presence of peripheral neurons (Fig. 4B). Additionally, the identity of the converted neurons was differentially altered according to the extrinsic patterning. We observed that SB-LDN patterning, when combined with NGN2 conversion, was an effective strategy for generating an enriched culture of forebrain cortical neurons. Both SB-LDN-NGN2 and NGN2 conditions converted hESCs towards a cortical identity (Fig. 4B, D), however, SB-LDN patterning produced a more pure population of forebrain neurons, whereas the NGN2 alone could also produce peripheral neurons (Fig. 3D); RNAseq analysis revealed expression of genes representative of broader brain regions (Fig. 4C). In accordance with this, the gene expression of forebrain markers *SIX3* and *FOXG1* in the SB-LDN-NGN2 group was significantly higher than in the NGN2 group, and the SB-LDN-NGN2 group had no detectable levels of the midbrain markers *PAX2*, *PAX5* or *EN1* (Fig. 4C).

Patterning of hESCs/iPSCs into hindbrain progenitors by treatment with SB431542 and CHIR for 4 days, followed by NGN2 conversion, generated anterior hindbrain excitatory neurons (Fig. 4). *VSX2* was seen to be significantly upregulated in the SB-CHIR-NGN2 group and we could detect an abundance of these neurons within the culture (Fig. 4G). VSX2 is a transcription factor and, within the hindbrain and spinal cord, it is specific to V2a interneuron (Al-Mosawie et al., 2007; Clovis et al., 2016; Li et al., 2005; Lundfald et al., 2007). To further confirm the identity of the interneuron, we examined the expression of SHOX2 by immunostaining, which co-localized with VSX2. Significantly more transcripts for *SHOX2* were also detected in the SB-CHIR-NGN2 group. Interestingly, we observed that not all VSX2 interneurons expressed SHOX2. Neurons double-positive for VSX2 and SHOX2 are known to be excitatory interneurons that control motor neurons, while the $VSX2^{+}SHOX2^{-}$ activate the commissural pathways involved in left–right coordination. (Dougherty et al., 2013; Ha and Dougherty, 2018).

A recent study demonstrates that V2a interneurons can be differentiated from human PSCs by dual SMAD inhibition, followed by retinoic acid and low concentrations of a Smoothened agonist, and Notch inhibition (Butts et al., 2017). By contrast, we obtained V2a interneurons without the inclusion of extrinsic factors to specifically activate the SHH pathway, which suggests that some basal plate SHH targets may be activated directly by the NGN2 conversion. In accordance with this, Ngn2 is regionally expressed in the basal plate of the developing mouse spinal cord and has been shown to be involved in regulating the expression of ventral transcription factors (Scardigli et al., 2001). The neuralizing transcription factor in direct conversion protocols may therefore also influence the neuronal subtypes generated. Furthermore, in direct conversion experiments NGN2 has been shown to preferentially give rise to excitatory neurons. As expected, by inhibiting the AMPA receptor, we found that indeed excitatory neurons were the main neuronal cell type present in all of our iN groups (Fig. 6 and Supplementary Fig. 4).

The Notch pathway has previously been shown to control the specification between V2a and V2b interneurons, with Notch inhibition specifying V2a over V2b interneurons (Del Barrio et al., 2007; Peng

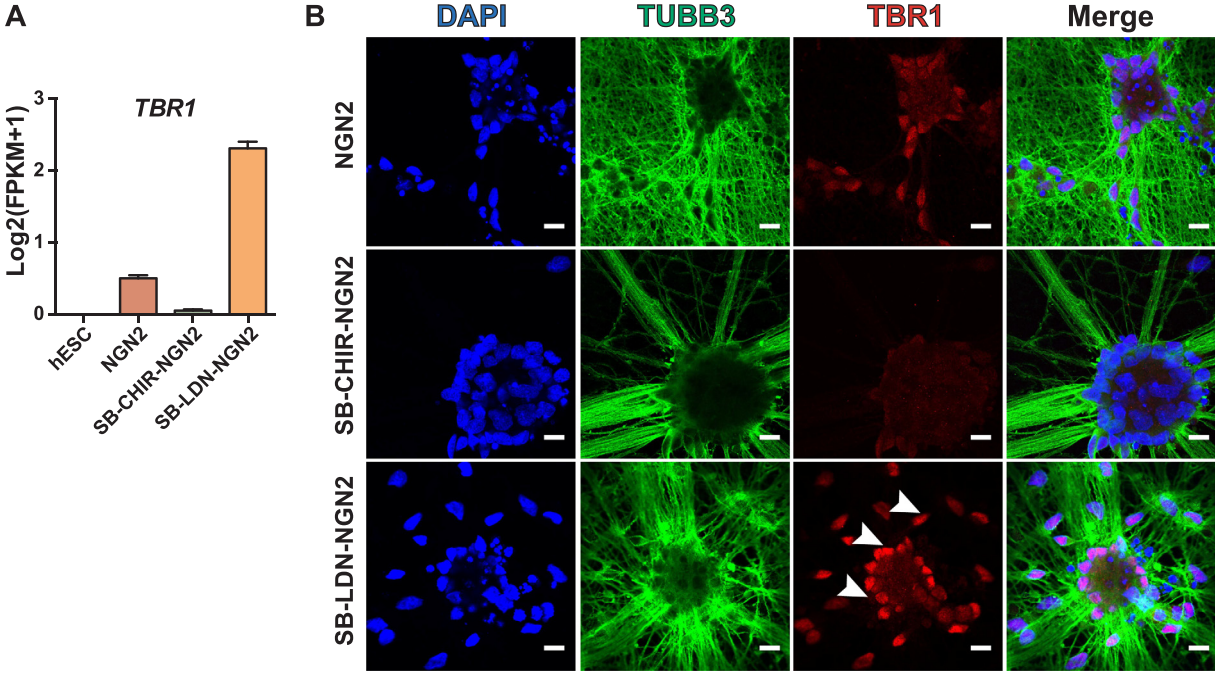

Fig. 5. The gene expression profile and immunostaining images of cortical marker TBR1. (A) Expression level profiling of cortical marker, TBR1 in hESC, NGN2, SB-CHIR-NGN2 and SB-LDN-NGN2 groups. FPKM + 1 values log2 transformed and plotted as mean with S.D, n = 3. (B) Representative images of DAPI, TUBB3, and TBR1 staining. Arrowheads point to representative TBR1 positive cells. Bar = 10 μm.

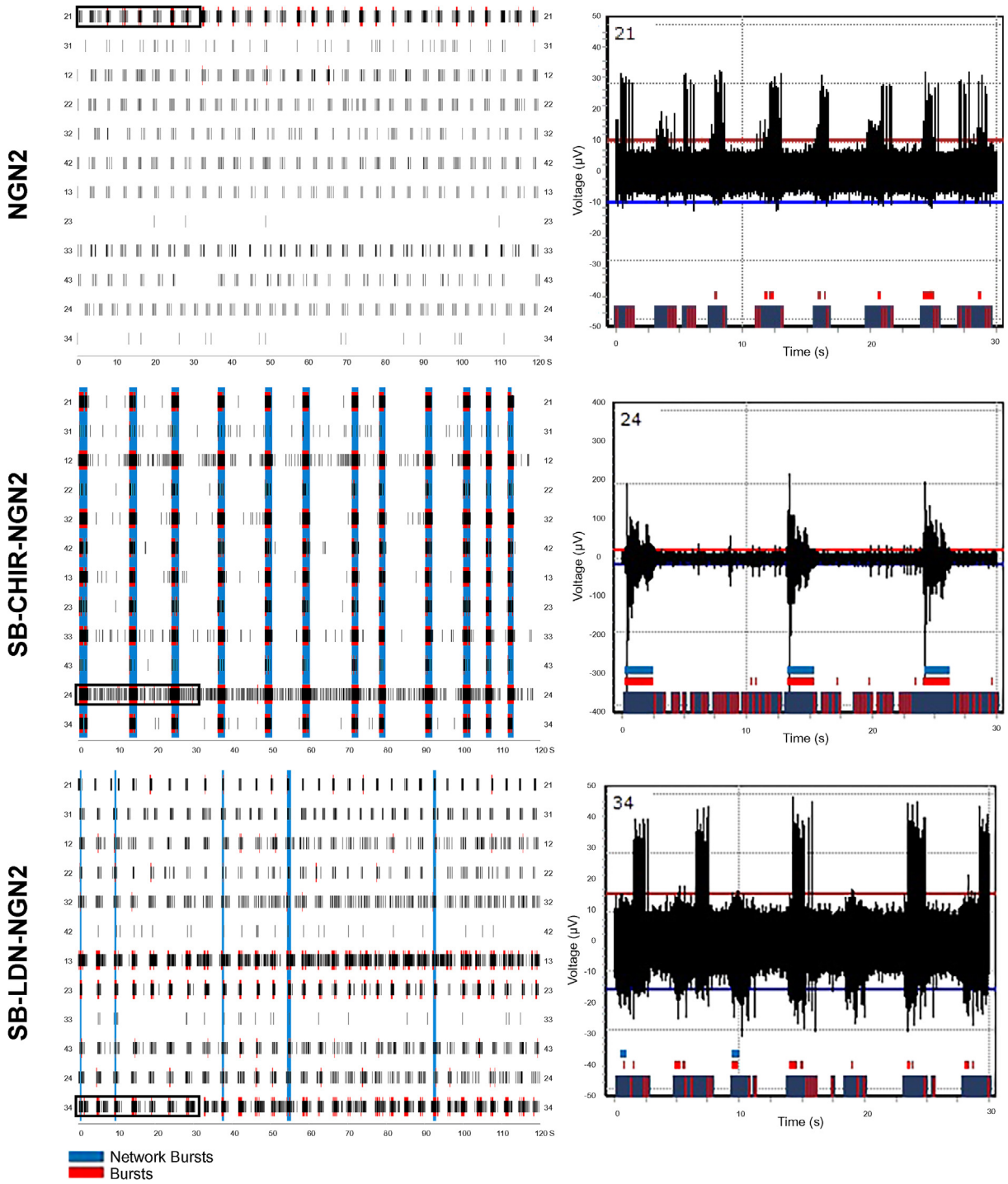

Fig. 6. Electrophysiological activities of the three iN groups by multi-electrode array (MEA). Raster plots of spontaneous activities for 2 mins (left, x axis is time and y axis is channel ID) and 30 s (right, numbers in the corners of boxed plots are the channel IDs) of raw data from the representative electrodes on week 7. Each black line represents a spike detection. Each red line represents a single channel burst (a collection of at least 4 spikes). Each blue line represents a network burst detection (with minimum of 50% of participating electrodes across entire well and minimum 25% of simultaneous channels). The images on the right side were 30 s recording from the left (marked with black rectangles).

et al., 2007). In all of our iN groups, we could not detect *GATA3* expression, a marker of V2b interneurons. DAPT was also included during the NGN2 conversion, to enhance neuronal conversion, which in combination with NGN2 likely helped promote the specification of V2a over V2b cell types. This suggests that the influence of patterning factors, specifically DAPT, on the neuronal subtypes would also be effective during the later NGN2 conversion phase. Indeed, simultaneous patterning and neuronal conversion from either fibroblasts or iPSCs can result in a more robust conversion and with the inclusion of dual SMAD factors and WNT antagonists enhance the specification of forebrain neurons (Ladewig et al., 2012; Nehme et al., 2018).

In conclusion, we demonstrated that sequential patterning and neuronal conversion of human PSCs is a highly successful method for manipulating the identity of the neurons with the ability to regionally specify them along the rostral caudal axis, which results in a more defined population of neurons. This approach can be used for

investigating a range of neurological disorders such as AD, MND or spinal cord injury.

CRediT authorship contribution statement

Muwan Chen: Methodology, Investigation, Data curation, Formal analysis, Writing - original draft, Writing - review & editing, Funding acquisition. **Muyesier Maimaitili:** Investigation. **Mette Habekost:** Formal analysis. **Katherine P. Gill:** Investigation. **Noëmie Mermet-Joret:** Investigation, Formal analysis. **Sadegh Nabavi:** Formal analysis. **Fabia Febbraro:** Investigation, Writing - review & editing. **Mark Denham:** Conceptualization, Methodology, Formal analysis, Supervision, Writing - review & editing, Funding acquisition.

Declaration of Competing Interest

The authors declare that they have no known competing financial interests or personal relationships that could have appeared to influence the work reported in this paper.

Acknowledgements

We thank Susanne Hvolbøl Buchholdt for assistance in iPSC maintenance. Patient fibroblasts used to generate iPSCs were obtained from: the Neuro-Biobank of the University of Tuebingen, Germany (http://www.hihtuebingen.de/nd/biobank/for-researchers/), which is supported by the Hertie Institute and the DZNE; the "Cell Line and DNA Biobank from Patients affected by Genetic Diseases" (Istituto G. Gaslini); and the "Parkinson Institute Biobank" (Milan, http://www.parkinsonbiobank.com/), which are members of the Telethon Network of Genetic Biobanks (project no. GTB12001), funded by Telethon Italy.

Funding: This study was supported by Lundbeckfonden grant no. DANDRITE-R248-2016-2518 and the Parkinsonforeningen. MC is supported by a postdoctoral fellowship from the Lundbeckfonden grant no. R209-2015-3100. MD is a partner of BrainStem—Stem Cell Center of Excellence in Neurology, funded by Innovation Fund Denmark.

Appendix A. Supplementary data

Supplementary data to this article can be found online at https://doi.org/10.1016/j.scr.2020.101945.

References

Al-Mosawie, A., Wilson, J.M., Brownstone, R.M., 2007. Heterogeneity of V2-derived interneurons in the adult mouse spinal cord. Eur. J. Neurosci. 26, 3003–3015. https://doi.org/10.1111/j.1460-9568.2007.05907.x.

Ambasudhan, R., Talantova, M., Coleman, R., Yuan, X., Zhu, S., Lipton, S.A., Ding, S., 2011. Direct reprogramming of adult human fibroblasts to functional neurons under defined conditions. Cell Stem Cell 9, 113–118. https://doi.org/10.1016/j.stem.2011.07.002.

Arenas, E., Denham, M., Villaescusa, J.C., 2015. How to make a midbrain dopaminergic neuron. Development 142, 1918–1936. https://doi.org/10.1242/dev.097394.

Blanchard, J.W., Eade, K.T., Szűcs, A., Lo Sardo, V., Tsunemoto, R.K., Williams, D., Sanna, P.P., Baldwin, K.K., 2014. Selective conversion of fibroblasts into peripheral sensory neurons. Nat. Neurosci. 18, 25–35. https://doi.org/10.1038/nn.3887.

Butts, J.C., McCreedy, D.A., Martinez-Vargas, J.A., Mendoza-Camacho, F.N., Hookway, T.A., Gifford, C.A., Taneja, P., Noble-Haeusslein, L., McDevitt, T.C., 2017. Differentiation of V2a interneurons from human pluripotent stem cells. Proc. Natl. Acad. Sci. 114, 4969–4974. https://doi.org/10.1073/pnas.1608254114.

Chambers, S.M., Qi, Y., Mica, Y., Lee, G., Zhang, X., Niu, L., Bilsland, J., Cao, L., Stevens, E., Whiting, P., Shi, S., Studer, L., 2012. Combined small-molecule inhibition accelerates developmental timing and converts human pluripotent stem cells into nociceptors. Nat. Biotechnol. 30, 715–720. https://doi.org/10.1038/nbt.2249.

Chanda, S., Ang, C.E., Davila, J., Pak, C., Mall, M., Lee, Q.Y., Ahlenius, H., Jung, S.W., Südhof, T.C., Wernig, M., 2014. Generation of induced neuronal cells by the single reprogramming factor ASCL1. Stem Cell Reports 3, 282–296. https://doi.org/10.1016/j.stemcr.2014.05.020.

Chen, M., Laursen, S.H., Habekost, M., Knudsen, C.H., Buchholdt, S.H., Huang, J., Xu, F., Liu, X., Bolund, L., Luo, Y., Nissen, P., Febbraro, F., Denham, M., 2018. Central and peripheral nervous system progenitors derived from human pluripotent stem cells reveal a unique temporal and cell-type specific expression of PMCAs. Front. Cell Dev. Biol. 6. https://doi.org/10.3389/fcell.2018.00005.

Chen, M., Maimaitili, M., Buchholdt, S.H., Jensen, U.B., Febbraro, F., Denham, M., 2020a. Generation of eight human induced pluripotent stem cell lines from Parkinson's disease patients carrying familial mutations. Stem Cell Res. 42, 101657. https://doi.org/10.1016/j.scr.2019.101657.

Chen, M., Maimaitili, M., Buchholdt, S.H., Jensen, U.B., Febbraro, F., Denham, M., 2020b. Generation of an induced pluripotent stem cell line (DANi-011A) from a Parkinson's disease patient with a LRRK2 p. G2019S mutation. Stem Cell Res. 45, 101781. https://doi.org/10.1016/j.scr.2020.101781.

Clovis, Y.M., Seo, S.Y., Kwon, J. sun, Rhee, J.C., Yeo, S., Lee, J.W., Lee, S., Lee, S.K., 2016. Chx10 consolidates V2a interneuron identity through two distinct gene repression modes. Cell Rep. 16, 1642–1652. https://doi.org/10.1016/j.celrep.2016.06.100.

Davis-Dusenbery, B.N., Williams, L.A., Klim, J.R., Eggan, K., 2014. How to make spinal motor neurons. Development 141, 491–501. https://doi.org/10.1242/dev.097410.

Del Barrio, M.G., Taveira-Marques, R., Muroyama, Y., Yuk, D.-I., Li, S., Wines-Samuelson, M., Shen, J., Smith, H.K., Xiang, M., Rowitch, D., Richardson, W.D., 2007. A regulatory network involving Foxn4, Mash1 and delta-like 4/Notch1 generates V2a and V2b spinal interneurons from a common progenitor pool. Development 134, 3427–3436. https://doi.org/10.1242/dev.005868.

Denham, M., Bye, C., Leung, J., Conley, B.J., Thompson, L.H., Dottori, M., 2012. Glycogen synthase kinase 3β and activin/nodal inhibition in human embryonic stem cells induces a pre-neuroepithelial state that is required for specification to a floor plate cell lineage. Stem Cells 30, 2400–2411. https://doi.org/10.1002/stem.1204.

Denham, M., Hasegawa, K., Menheniott, T., Rollo, B., Zhang, D., Hough, S., Alshawaf, A., Febbraro, F., Ighaniyan, S., Leung, J., Elliott, D.A., Newgreen, D.F., Pera, M.F., Dottori, M., 2015. Multipotent caudal neural progenitors derived from human pluripotent stem cells that give rise to lineages of the central and peripheral nervous system. Stem Cells 33, 1759–1770. https://doi.org/10.1002/stem.1991.

Dougherty, K.J., Zagoraiou, L., Satoh, D., Rozani, I., Doobar, S., Arber, S., Jessell, T.M., Kiehn, O., 2013. Locomotor rhythm generation linked to the output of spinal Shox2 excitatory interneurons. Neuron 80, 920–933. https://doi.org/10.1016/j.neuron.2013.08.015.

Goparaju, S.K., Kohda, K., Ibata, K., Soma, A., Nakatake, Y., Akiyama, T., Wakabayashi, S., Matsushita, M., Sakota, M., Kimura, H., Yuzaki, M., Ko, S.B.H., Ko, M.S.H., 2017. Rapid differentiation of human pluripotent stem cells into functional neurons by mRNAs encoding transcription factors. Sci. Rep. 7, 1–12. https://doi.org/10.1038/srep42367.

Ha, N.T., Dougherty, K.J., 2018. Spinal Shox2 interneuron interconnectivity related to function and development. Elife 7. https://doi.org/10.7554/eLife.42519.

Ladewig, J., Mertens, J., Kesavan, J., Doerr, J., Poppe, D., Glaue, F., Herms, S., Wernet, P., Kögler, G., Müller, F.-J., Koch, P., Brüstle, O., 2012. Small molecules enable highly efficient neuronal conversion of human fibroblasts. Nat. Methods 9, 575–578. https://doi.org/10.1038/nmeth.1972.

Li, S., Misra, K., Matise, M.P., Xiang, M., 2005. Foxn4 acts synergistically with Mash1 to specify subtype identity of V2 interneurons in the spinal cord. Proc. Natl. Acad. Sci. 102, 10688–10693. https://doi.org/10.1073/pnas.0504799102.

Lundfald, L., Restrepo, C.E., Butt, S.J.B., Peng, C.-Y., Droho, S., Endo, T., Zeilhofer, H.U., Sharma, K., Kiehn, O., 2007. Phenotype of V2-derived interneurons and their relationship to the axon guidance molecule EphA4 in the developing mouse spinal cord. Eur. J. Neurosci. 26, 2989–3002. https://doi.org/10.1111/j.1460-9568.2007.05906.x.

Nehme, R., Zuccaro, E., Ghosh, S.D., Li, C., Sherwood, J.L., Pietilainen, O., Barrett, L.E., Limone, F., Worringer, K.A., Kommineni, S., Zang, Y., Cacchiarelli, D., Meissner, A., Adolfsson, R., Haggarty, S., Madison, J., Muller, M., Arlotta, P., Fu, Z., Feng, G., Eggan, K., 2018. Combining NGN2 programming with developmental patterning generates human excitatory neurons with NMDAR-mediated synaptic transmission. Cell Rep. 23, 2509–2523. https://doi.org/10.1016/j.celrep.2018.04.066.

Pang, Z.P., Yang, N., Vierbuchen, T., Ostermeier, A., Fuentes, D.R., Yang, T.Q., Citri, A., Sebastiano, V., Marro, S., Sudhof, T.C., Wernig, M., 2011. Induction of human neuronal cells by defined transcription factors. Nature 476, 220–223. https://doi.org/10.1038/nature10202.

Peng, C.Y., Yajima, H., Burns, C.E., Zon, L.I., Sisodia, S.S., Pfaff, S.L., Sharma, K., 2007. Notch and MAML signaling drives Scl-dependent interneuron diversity in the spinal cord. Neuron 53, 813–827. https://doi.org/10.1016/j.neuron.2007.02.019.

Pfisterer, U., Kirkeby, A., Torper, O., Wood, J., Nelander, J., Dufour, A., Björklund, A., Lindvall, O., Jakobsson, J., Parmar, M., 2011. Direct conversion of human fibroblasts to dopaminergic neurons. Proc. Natl. Acad. Sci. U.S.A. 108, 10343–10348. https://doi.org/10.1073/pnas.1105135108.

Qi, Y., Zhang, X.-J., Renier, N., Wu, Z., Atkin, T., Sun, Z., Ozair, M.Z., Tchieu, J., Zimmer, B., Fattahi, F., Ganat, Y., Azevedo, R., Zeltner, N., Brivanlou, A.H., Karayiorgou, M., Gogos, J., Tomishima, M., Tessier-Lavigne, M., Shi, S.-H., Studer, L., 2017. Combined small-molecule inhibition accelerates the derivation of functional cortical neurons from human pluripotent stem cells. Nat. Biotechnol. 35. https://doi.org/10.1038/nbt.3777.

Scardigli, R., Schuurmans, C., Gradwohl, G., Guillemot, F., 2001. Crossregulation between Neurogenin2 and pathways specifying neuronal identity in the spinal cord. Neuron 31, 203–217. https://doi.org/10.1016/S0896-6273(01)00358-0.

Son, E.Y., Ichida, J.K., Wainger, B.J., Toma, J.S., Rafuse, V.F., Woolf, C.J., Eggan, K., 2011. Conversion of mouse and human fibroblasts into functional spinal motor neurons. Cell Stem Cell 9, 205–218. https://doi.org/10.1016/j.stem.2011.07.014.

Telezhkin, V., Schnell, C., Yarova, P.L., Yung, S., Sanders, P., Cope, E., Hughes, A., Thompson, B.A., Geater, C., Hancock, J.M., Joy, S., Badder, L., Connor-Robson, N., Comella, A., Straccia, M., Bombau, G., Brown, J.T., Canals, J.M., Randall, A.D., Allen, N.D., Kemp, P.J., 2015. Forced cell-cycle exit and modulation of GABAA, CREB and

GSK3β signaling promote functional maturation of induced pluripotent stem cell-derived neurons. Am. J. Physiol. Cell Physiol., ajpcell.00166.2015. doi: 10.1152/ajpcell.00166.2015.

Theka, I., Caiazzo, M., Dvoretskova, E., Leo, D., Ungaro, F., Curreli, S., Managò, F., Dell'Anno, M.T., Pezzoli, G., Gainetdinov, R.R., Dityatev, A., Broccoli, V., 2013. Rapid generation of functional dopaminergic neurons from human induced pluripotent stem cells through a single-step procedure using cell lineage transcription factors. Stem Cells Transl. Med. 2, 473–479. https://doi.org/10.5966/sctm.2012-0133.

Thoma, E.C., Wischmeyer, E., Offen, N., Maurus, K., Sir??n, A.L., Schartl, M., Wagner, T. U., 2012. Ectopic expression of neurogenin 2 alone is sufficient to induce differentiation of embryonic stem cells into mature neurons. PLoS One 7. doi: 10.1371/journal.pone.0038651.

Vierbuchen, T., Ostermeier, A., Pang, Z.P., Kokubu, Y., Südhof, T.C., Wernig, M., 2010. Direct conversion of fibroblasts to functional neurons by defined factors. Nature 463, 1035–1041. https://doi.org/10.1038/nature08797.

Zhang, Y., Pak, C., Han, Y., Ahlenius, H., Zhang, Z., Chanda, S., Marro, S., Patzke, C., Acuna, C., Covy, J., Xu, W., Yang, N., Danko, T., Chen, L., Wernig, M., Südhof, T.C., 2013. Rapid single-step induction of functional neurons from human pluripotent stem cells. Neuron 78, 785–798. https://doi.org/10.1016/j.neuron.2013.05.029.